



Data Reduction Report

Jan 13, 2024

Contents

1	Final Light curve	1
1.1	Observation and processing summary	2
1.2	Noise curves and metrics	3
2	Summary of the processing stages	4
3	Processing summary	5
3.1	Bias correction	6
3.2	Gain correction	7
3.3	Non-linearity correction	8
3.4	Dark current correction	8
3.5	Flat field correction	9
3.6	Bad pixels correction	10
3.7	Smear correction	11
3.8	Background correction	12
3.9	Centroids estimation	13
3.10	Flux correlations	14
3.11	Contamination Estimation	15
3.12	DRP Photometry	17
4	Appendix	22
4.1	Event flagging code	22
4.2	Data Reduction Pipeline release log summary	22

1 Final Light curve

The plot below shows the final light curve obtained with the aperture of radius $R=25$ pix. This corresponds to the former DEFAULT aperture of previous DRP versions. All the analysis reported here corresponds to this aperture ($R=25$ pix) if not mention otherwise.

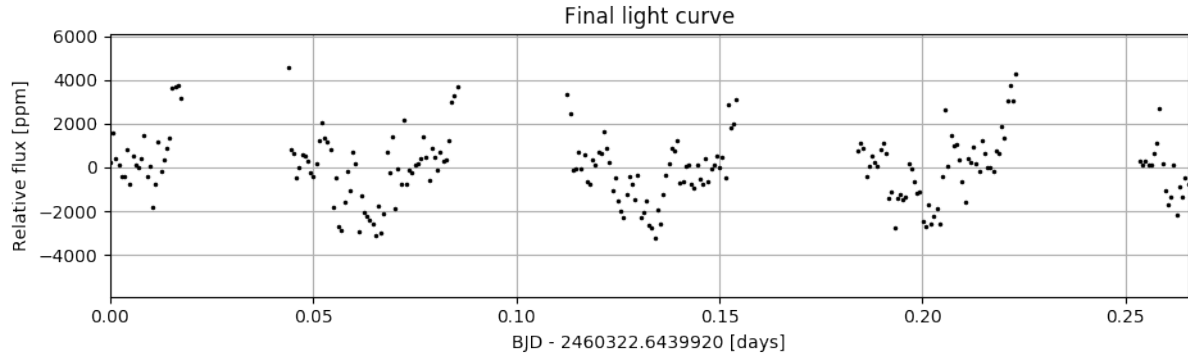


Figure 1. Final light curve of the observation corresponding to the DEFAULT (R=25 pix) aperture size. Only non-flagged points are shown.

1.1 Observation and processing summary

DPR run info	
Processing date	2024-01-13 19:00
Pipeline Version	14.1.3

TARGET	
Name	TOI5533
Teff [K]	7220.0
CHEOPS mag	11.09
GAIA G mag	11.09

PROGRAM	
PI	Hugh Osborn
PI ID	900051
Observation ID	2319976
Visit Number	1
Program Type	14
Program ID	9000
Request ID	89

Observation info	
Start [UTC]	2024-01-13 03:18
End [UTC]	2024-01-13 09:40
Duration [hrs]	6.37
Number of frames	224
Number of flagged frames	1
Integration time [s]	60.0
Repetition Period [s]	60.0
# Exposures x exp. time [s]	1 x 60.0 s
Imagettes available	No
Number of coadded imagettes	0.0
Stacking order of imagettes	0.0

Photometry info	
Aperture shape	Circular
Multi-aperture mode	Yes
Number of apertures	26
Aperture's radius range [pix]	15-40

Table 1. Summary of the observation and DRP run.

1.2 Noise curves and metrics

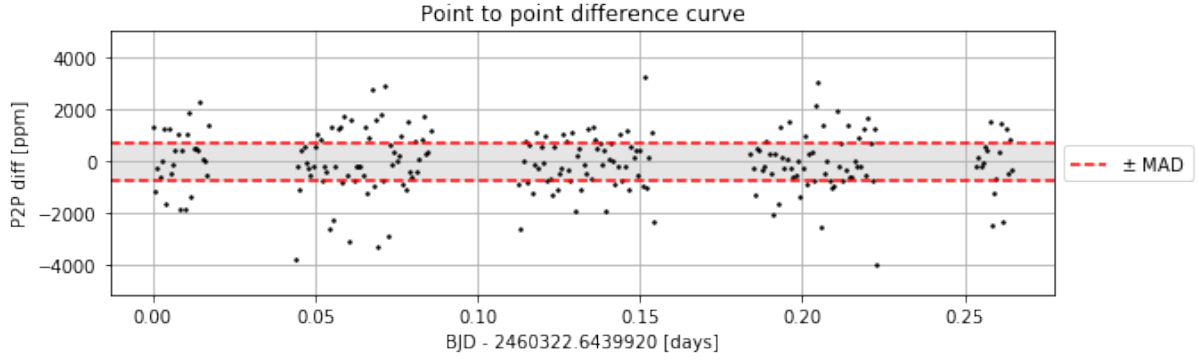


Figure 2. Difference between two consecutive points of the final light curve. Shaded area between dashed lines represents the median absolute deviation of the points (MAD).

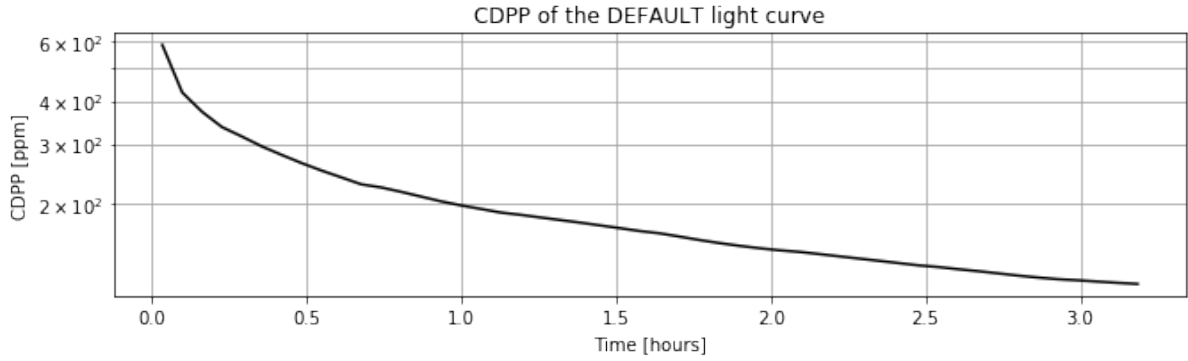


Figure 3. Combined Differential Photometric Precision (CDPP) estimation of the DEFAULT light curve. Only non-flagged points were considered for the CDPP estimation, therefore it might differ from the values recorded in the light curve headers where all the points were considered for the calculus. CDPP is estimated as in the DRP paper: [Hoyer et al. \(2020\)](#).

Light Curve Metrics	
Robust mean flux [e]	4.1926e+06
RMS [ppm]	1370
MAD [ppm]	803
CDPP 3h [ppm]	119
CDPP 6h [ppm]	104

Table 2. Metrics of the DEFAULT light curve using only non-flagged points. The CDPP of 3 and 6 hours (if apply) are given in the last two rows of the table.

2 Summary of the processing stages

DR Stage	Units	Mean	RMS
Bias	ADU/frame	6.28e+02	0.00e+00
RON	ADU/frame	3.50e+00	0.00e+00
Dark current	e-/pix/s	9.83e-01	0.00e+00
Gain	e-/ADU	1.95e+00	2.22e-16
Smear	e-/pix/s	2.83e-01	3.95e-01
Background	e-/pix/s	4.19e+00	1.71e+00

Table 3. Description of the quantities used for calibrating and correcting the data.

step	comments
bias	default value
gain	visit average value
linearization	combined from subarray and imagerettes
dark	from REF. file
cosmic rays	detection and correction
bad pixels	detection only
background	sky ring (radius=45-97pix)
smearing	model subtraction
contamination	modeled curve
photometry	circular mask

Table 4. Brief description of the source or method used to obtain each of the quantities adopted in the processing of the data. For detailed information please refer to the log files of the DRP.

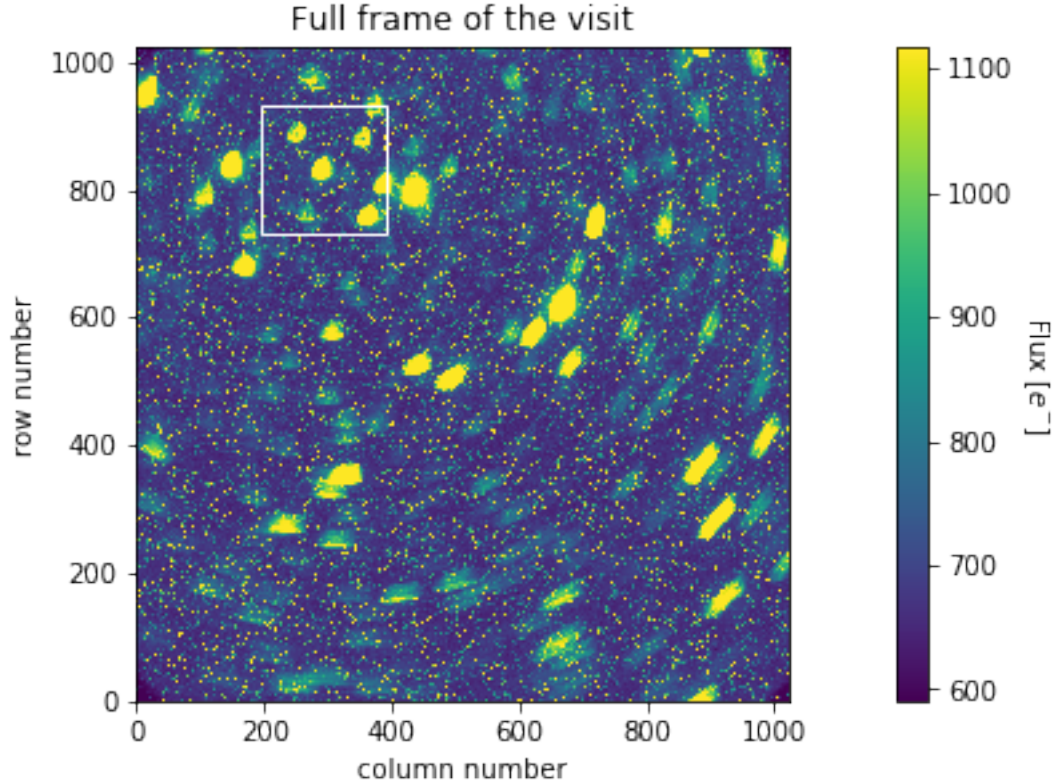


Figure 4. Field of view of the full (1024x1024 pix) CCD. The white square represents the location and size of the subarray window.

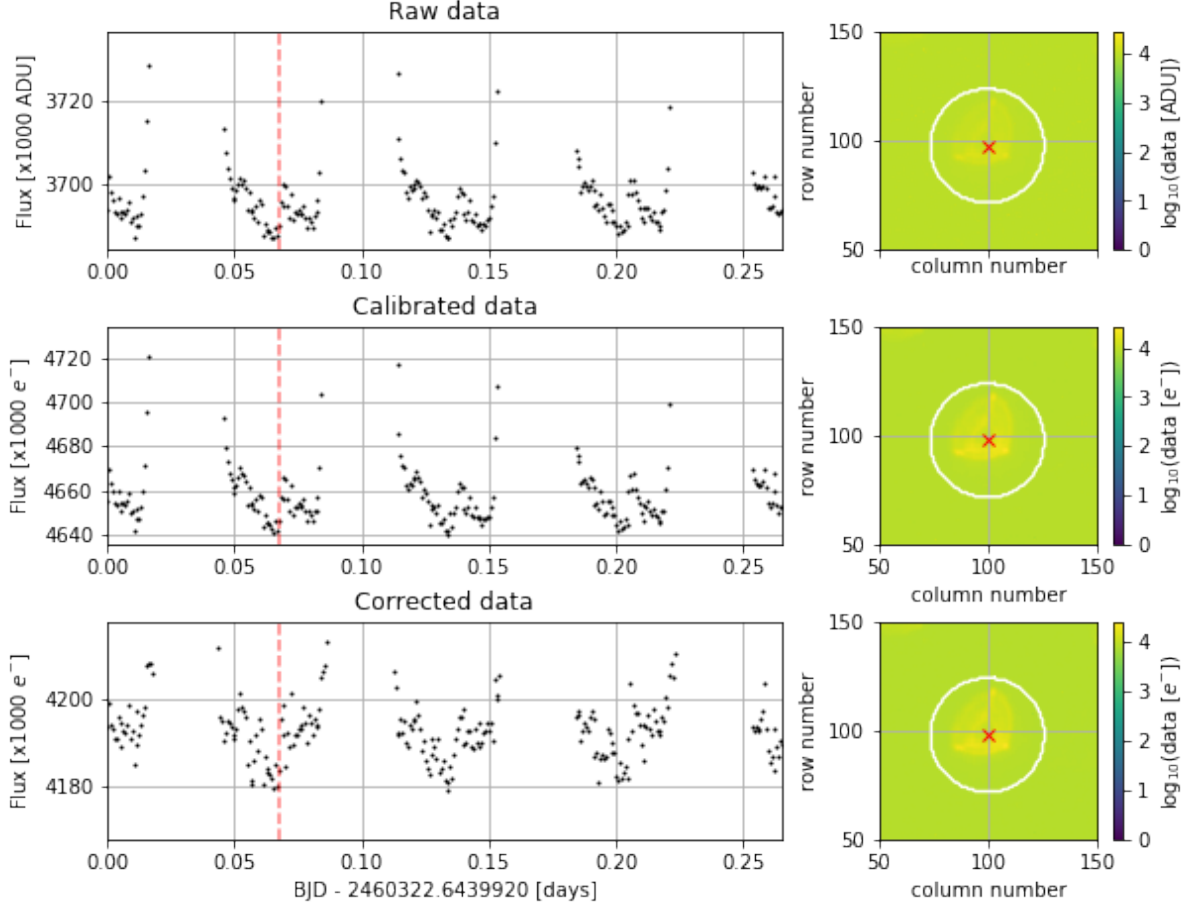


Figure 5. From top to bottom, raw, calibrated, and corrected data. Left: derived light curves after each of the main processing stages. Right: data snapshots of the corresponding processing level. The white circle and the red cross represent the DEFAULT photometric aperture and the estimated centroid, respectively. All points are shown including the flagged points but outliers are clipped for better visualization. The vertical dashed line in the left panel represents the corresponding time of the image shown at the right.

3 Processing summary

The following subsections present the relevant figures and derived light curves of each data processing step. In addition, a measure of the dispersion of the target's light curve before and after each step is given.

3.1 Bias correction

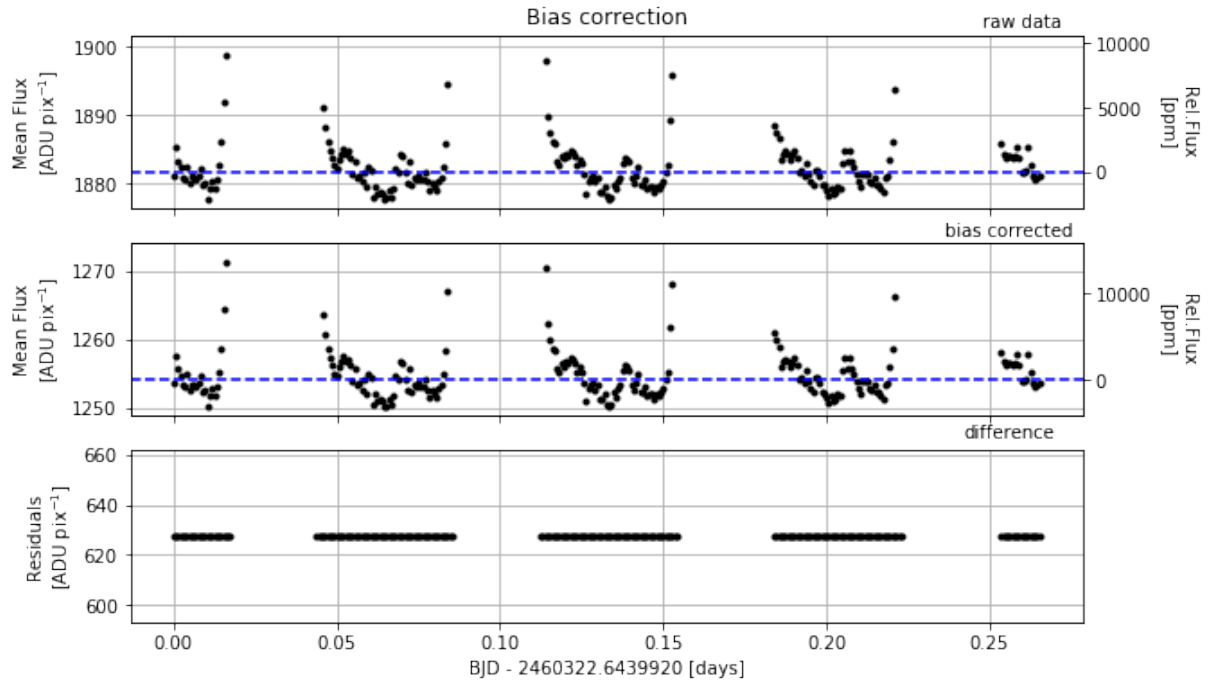


Figure 6. Light curves before (top) and after (middle) bias correction. The bottom plot shows the residuals after correction.

	Units	Mean	RMS
Residuals (bias)	ADU/pix/frame	627.60	0.00

Table 5. Mean and dispersion of the residuals after bias correction (bottom panel Figure 6). The values are computed in units of ADU/pix/number of stacked frames.

	p2p rms [ADU]	diff
before	4404.3	
after	4404.3	0.0

Table 6. Dispersion calculated over all the non-flagged points of the derived light curves before and after bias correction.

3.2 Gain correction

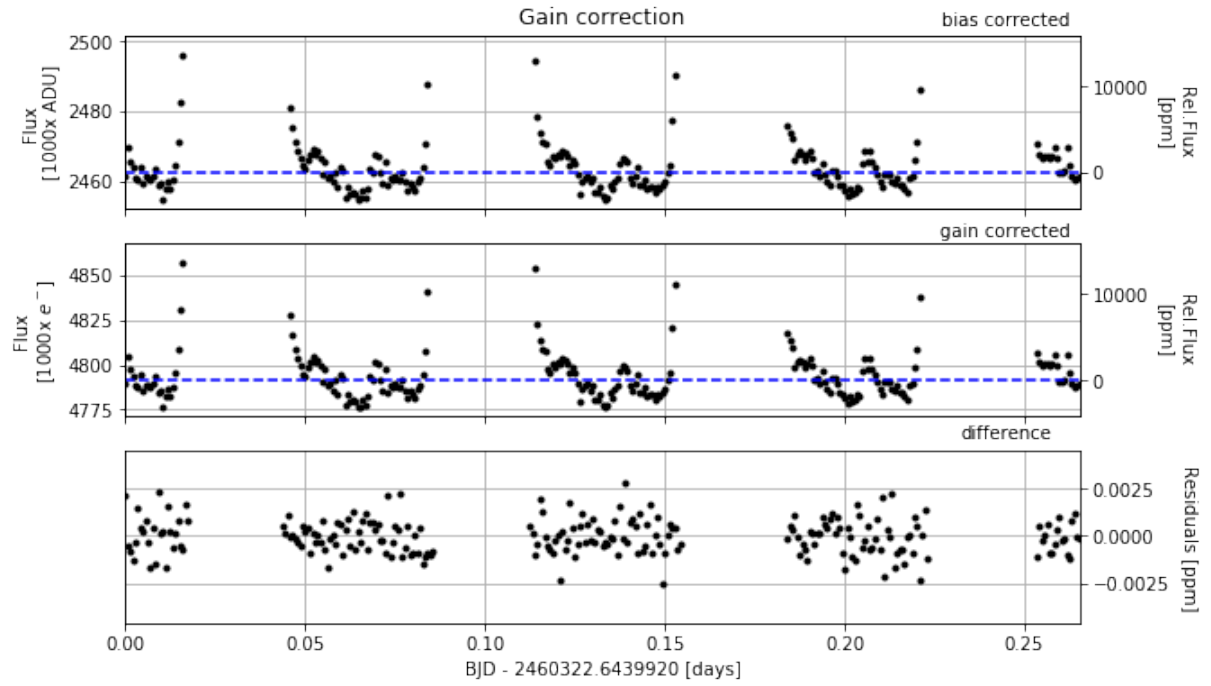


Figure 7. Light curves before (top) and after (middle) gain correction. Difference of the normalized light curves is shown at the bottom.

	Units	Mean	RMS
Residuals (GAIN)	[ppm]	-1.5e-05	9.2e-04

Table 7. Mean and dispersion of the residuals after gain correction (bottom panel Figure 7). The values are computed in units of ppm.

	p2p rms [ppm]	diff
before	42746.1	
after	42746.1	0.0

Table 8. Dispersion calculated over all the non-flagged points of the derived light curves before and after gain correction.

3.3 Non-linearity correction

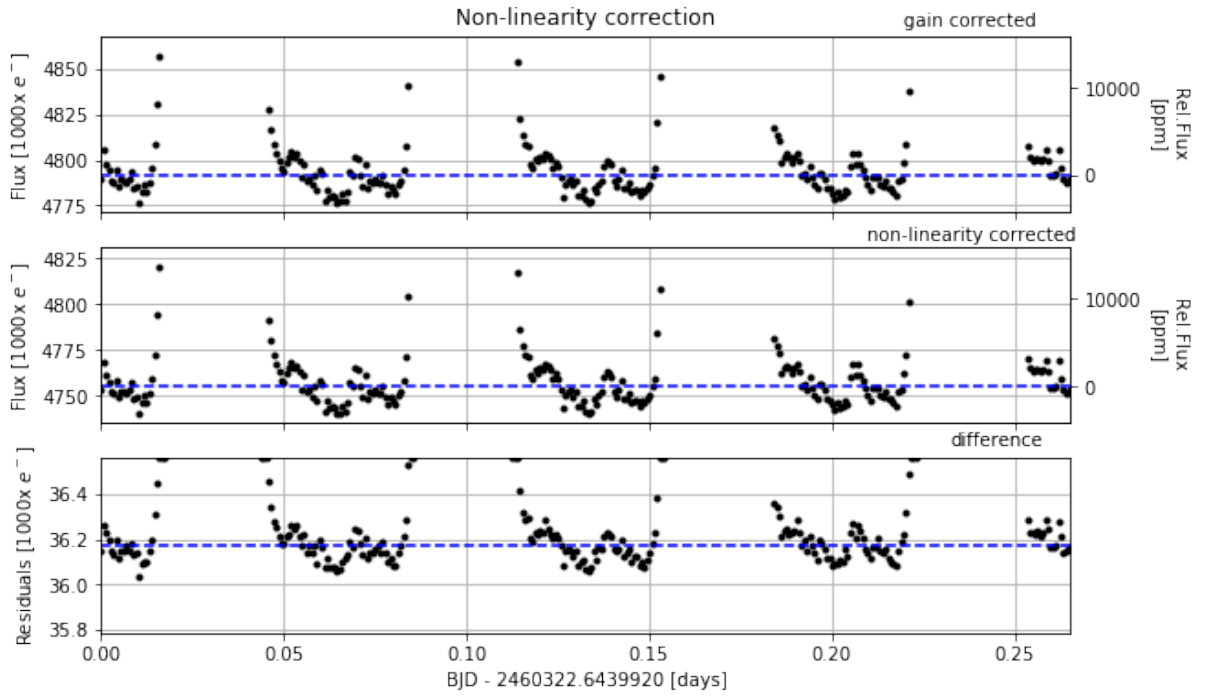


Figure 8. Light curves before (top) and after (middle) non-linearity correction. The difference of these light curves is shown in the bottom panel.

	p2p rms [e]	diff
before	8570.1	
after	8508.3	-61.757

Table 9. Dispersion of all non-flagged points of the derived light curves before and after non-linearity correction.

3.4 Dark current correction

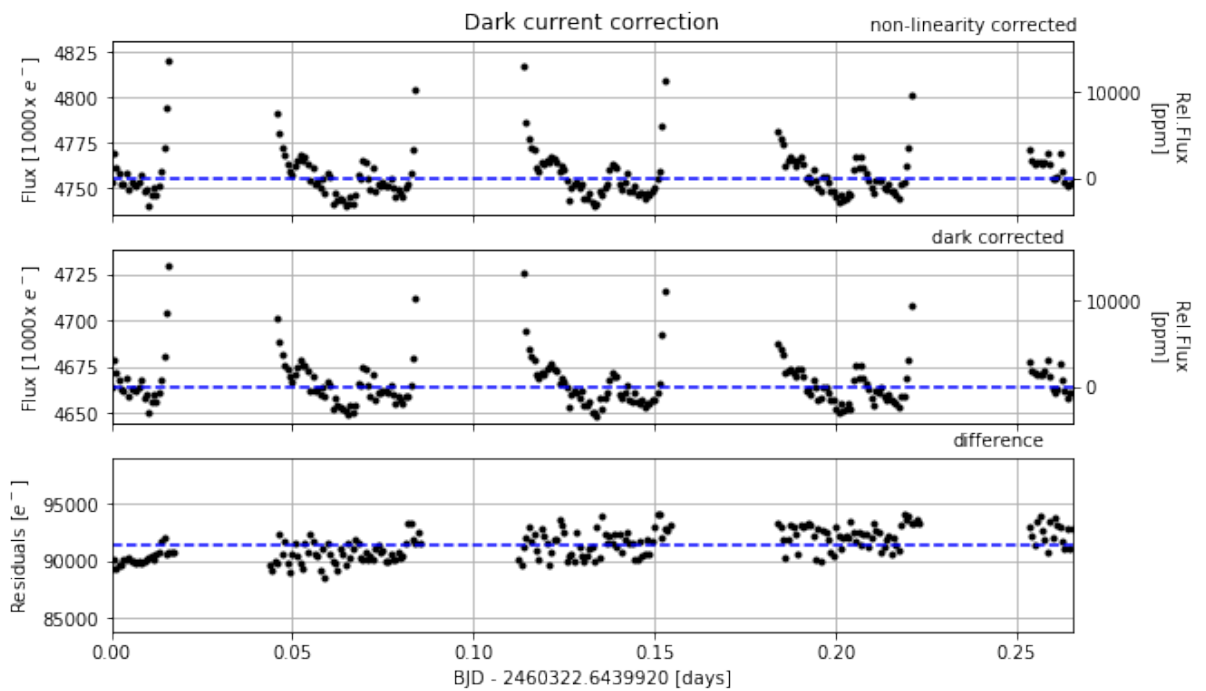


Figure 9. Light curves before (top) and after (middle) dark current correction. The difference of these light curves is shown in the bottom panel.

	Units	Mean	RMS
Residuals (DARK)	[e-]	91445.40	1265.47

Table 10: Mean and dispersion of the residuals after bias correction (bottom panel Figure 9). The values are computed in units of electron in the stacked frames for the full exposure time.

	p2p rms [e]	diff
before	8570.1	
after	8398.8	-171.312

Table 11. Dispersion of all non-flagged points of the derived light curves before and after dark correction.

3.5 Flat field correction

	Temperature [K]
Target T_eff	7220.0
Flat Field T_eff	7200.0

Table 12. Based on the provided temperature of the target (Target T_eff), the flat field correction was performed using the extension of the reference file corresponding to the temperature shown in the table (Flat Field T_eff).

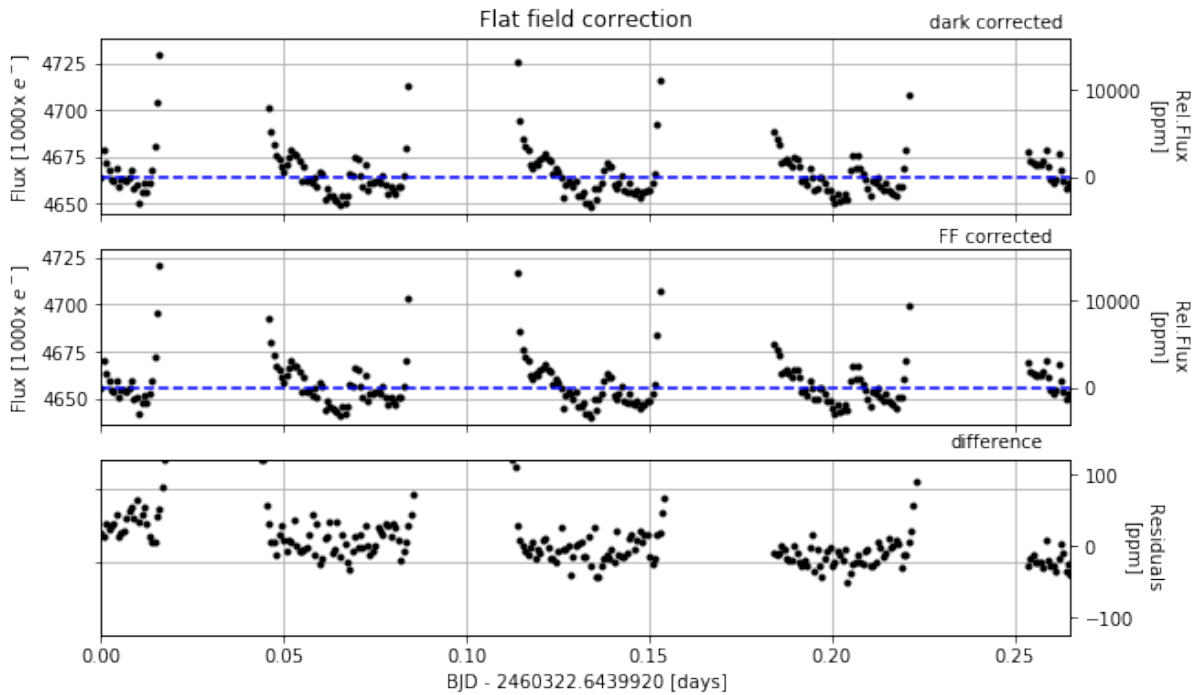


Figure 10. Light curves before (top) and after (middle) flat field correction. The difference between these light curves is shown in the bottom panel.

	p2p rms [ppm]	diff
before	48516.9	
after	48414.4	-102.43

Table 13. Dispersion of all the non-flagged points of the derived light curves before and after flat field correction.

3.6 Bad pixels correction

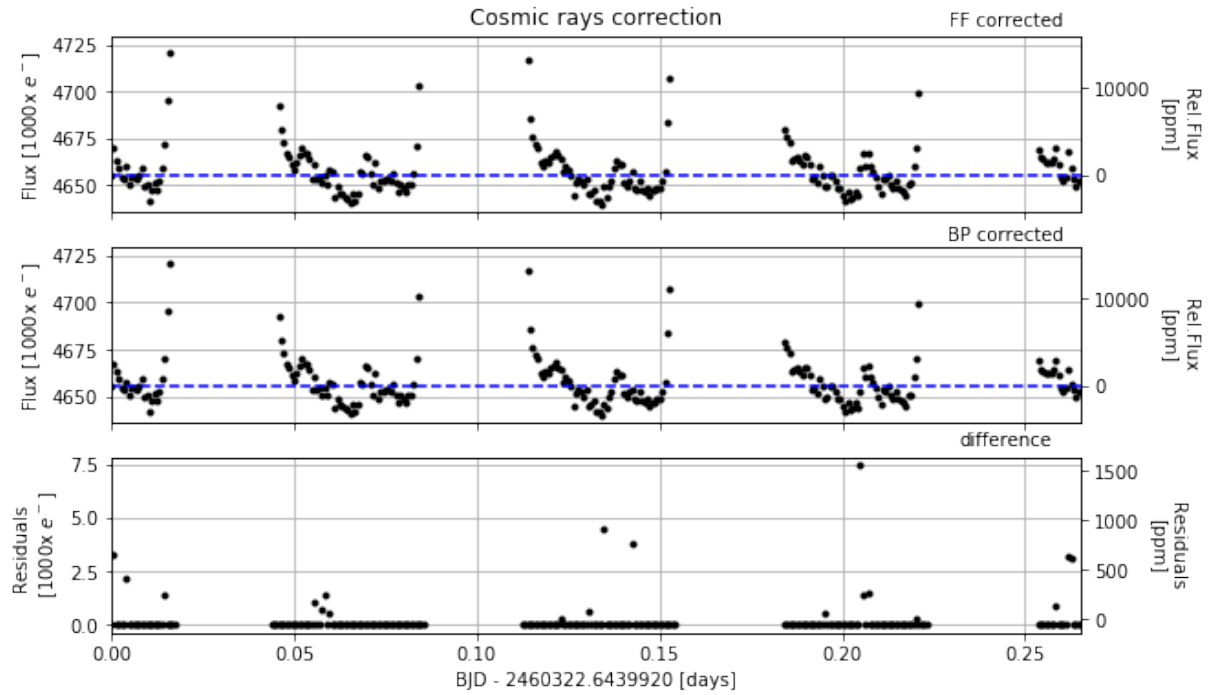


Figure 11. Light curves before (top) and after (middle) cosmic rays correction. The residuals are shown at the bottom. Only non-flagged points are shown in the plot.

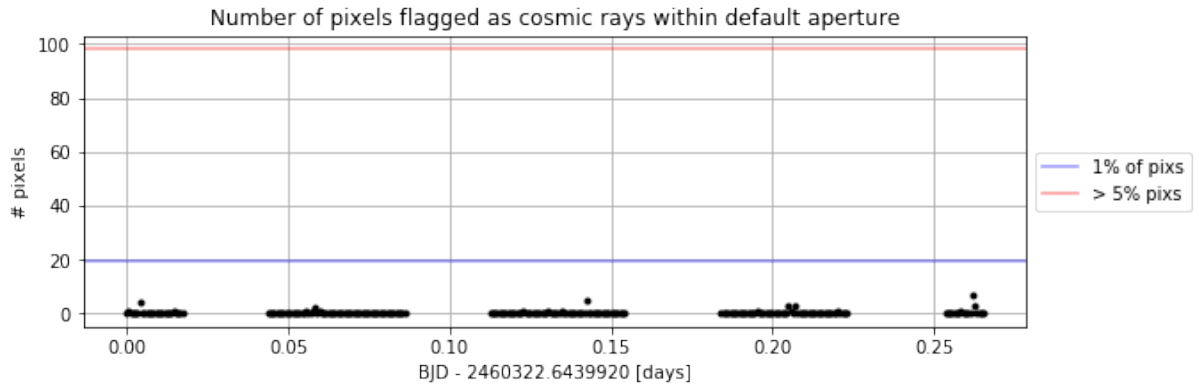


Figure 12. Number of pixels within the aperture affected by cosmic rays on each exposure. Blue line represents the 1% of the total number of pixels in the aperture. Points on the red line, when present, correspond to exposures with at least 5% of pixels affected by cosmic rays hits within the aperture. If present, vertical lines indicate the frames with more than 5% of the total number of pixels affected by cosmic rays (typically a good indicator of SAA crossings).

	p2p rms [ppm]	diff
before	48414.4	
after	48419.7	5.31

Table 14. Dispersion of all the non-flagged points of the derived light curves before and after cosmic rays correction.

3.7 Smear correction

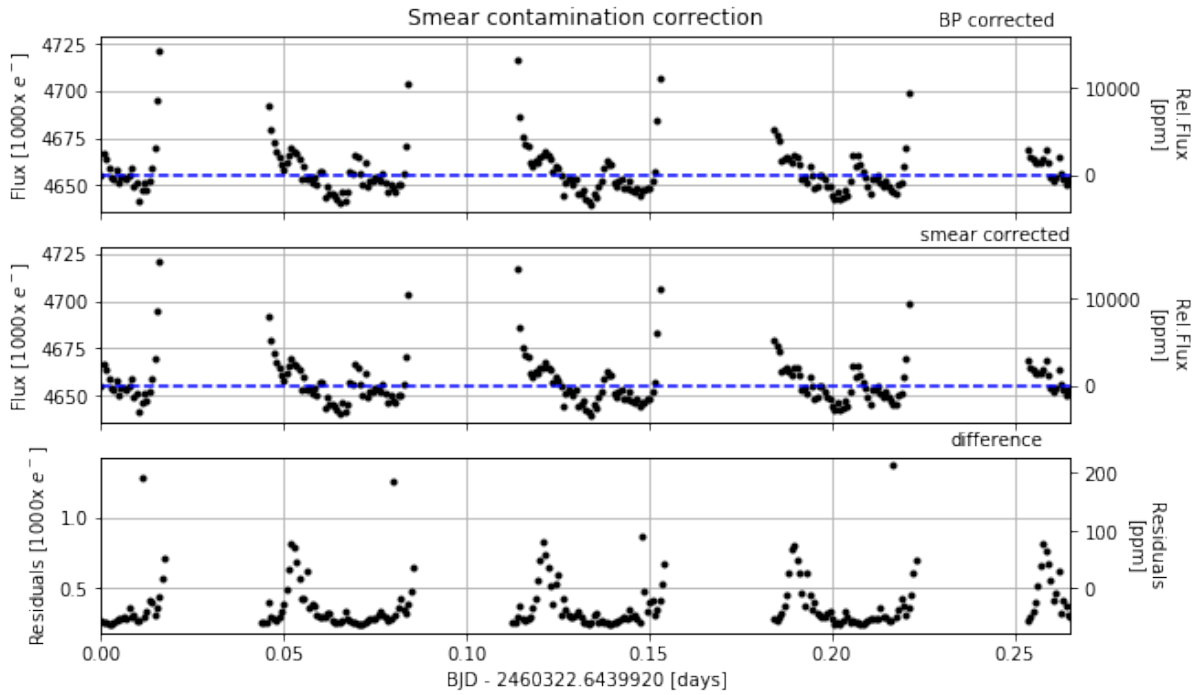


Figure 13. Light curves before (top) and after (middle) correction for smear contamination. The difference of the light curves is shown in the bottom panel.

	p2p rms [ppm]	diff
before	48419.7	
after	48420.8	1.03

Table 15. Dispersion of all the non-flagged points of the derived light curves before and after smear correction.

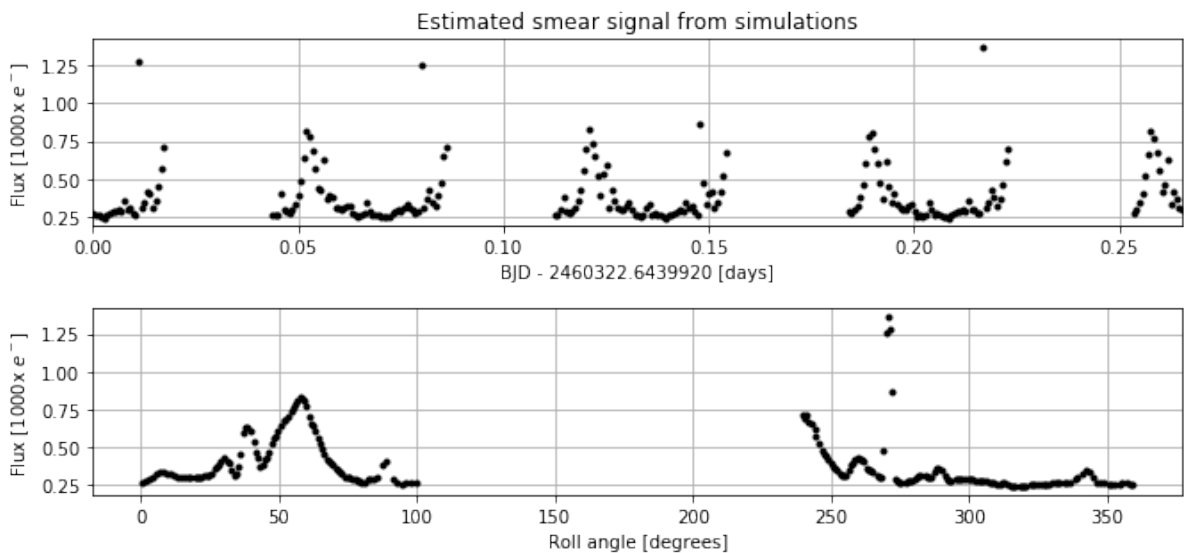


Figure 14. Light curve of the contribution of the smear trails estimated from the simulation of the visit (see section 3.11) as a function of time (top panel) and roll angle (bottom panel).

3.8 Background correction

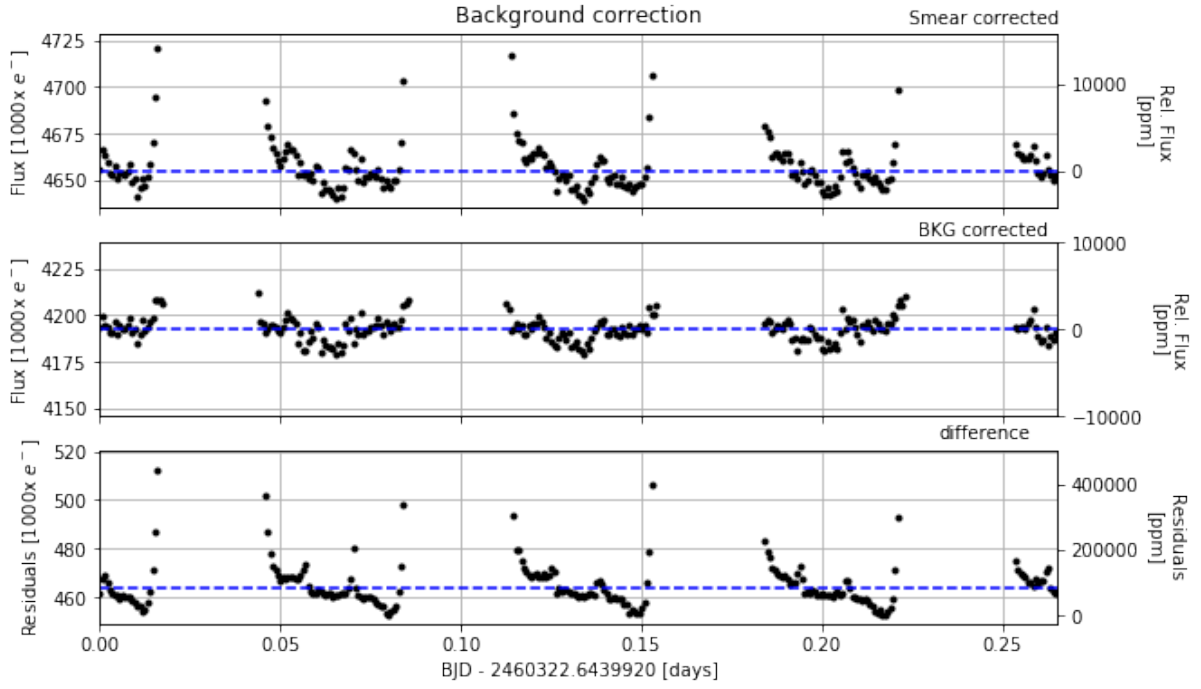


Figure 15. Light curves before (top) and after (middle) background correction. The difference is shown in the bottom panel.

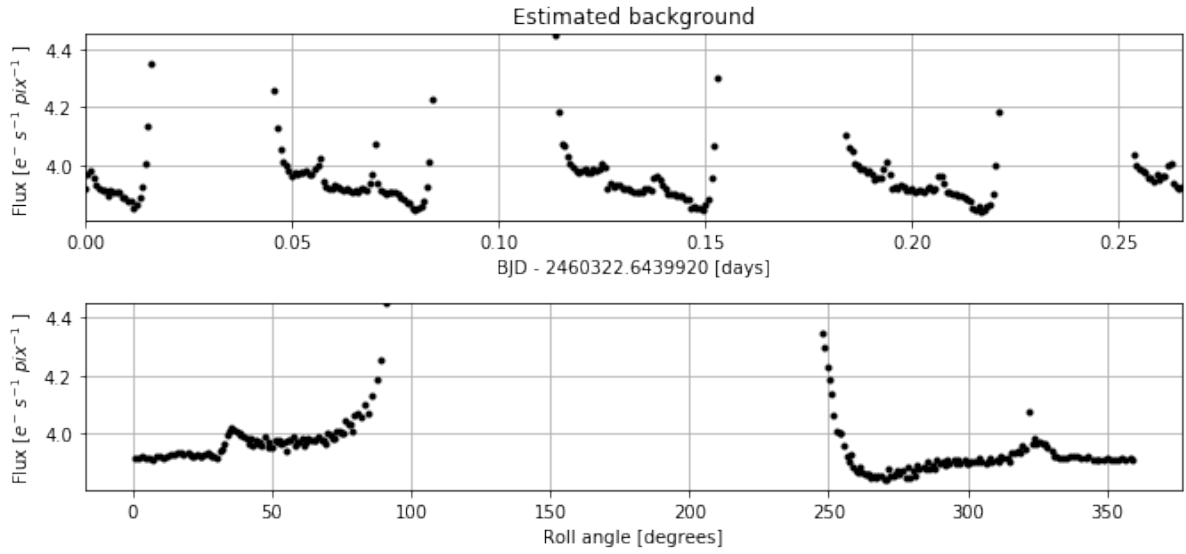


Figure 16. Estimated background signal per image as a function of time (top panel) and roll angle (bottom panel). The points are clipped for better visualization.

	p2p rms [ppm]	diff
before	48420.8	
after	1522.3	-46898.52

Table 16. Dispersion of all the non-flagged points of the derived light curves before and after background correction.

3.9 Centroids estimation

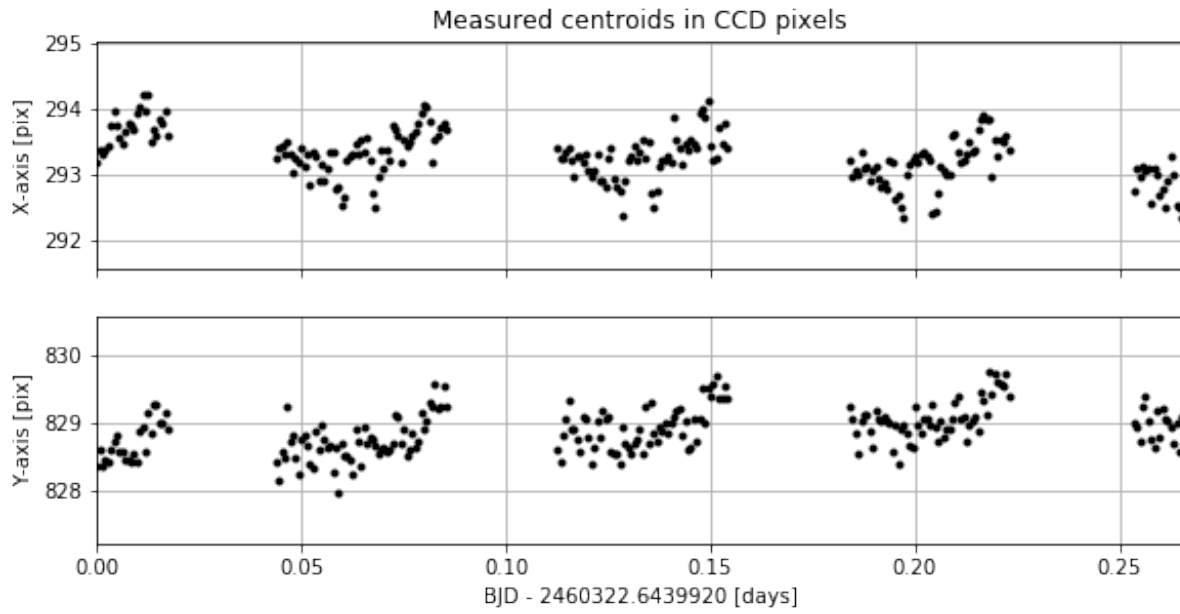


Figure 17. Estimated centroids in the X/Y-axis as a function of time. Pixels are referenced to the lower-left corner of the full CCD.

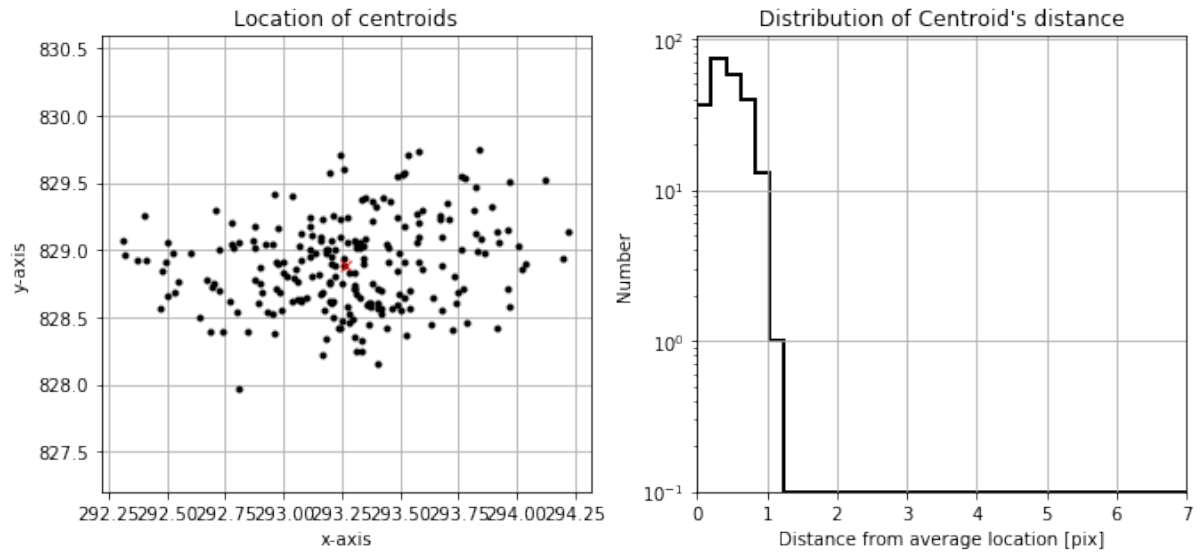


Figure 18. Left: location of the estimated centroids. The red cross represents the average value. Right: distribution of the distance of the centroids to the average estimated centroid.

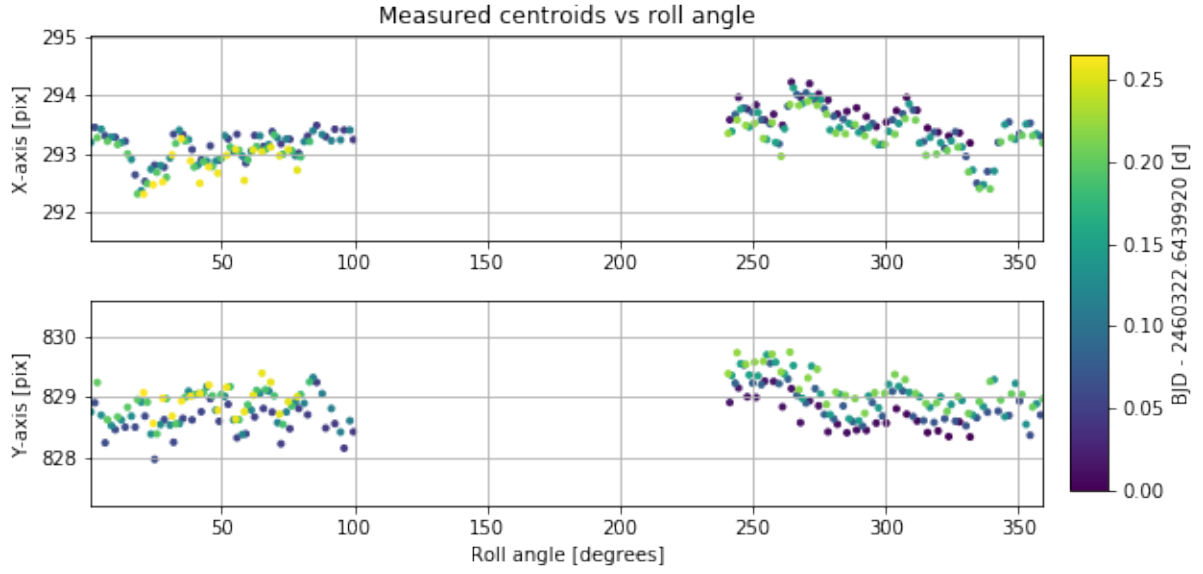


Figure 19. Centroids as a function of the roll angle.

3.10 Flux correlations

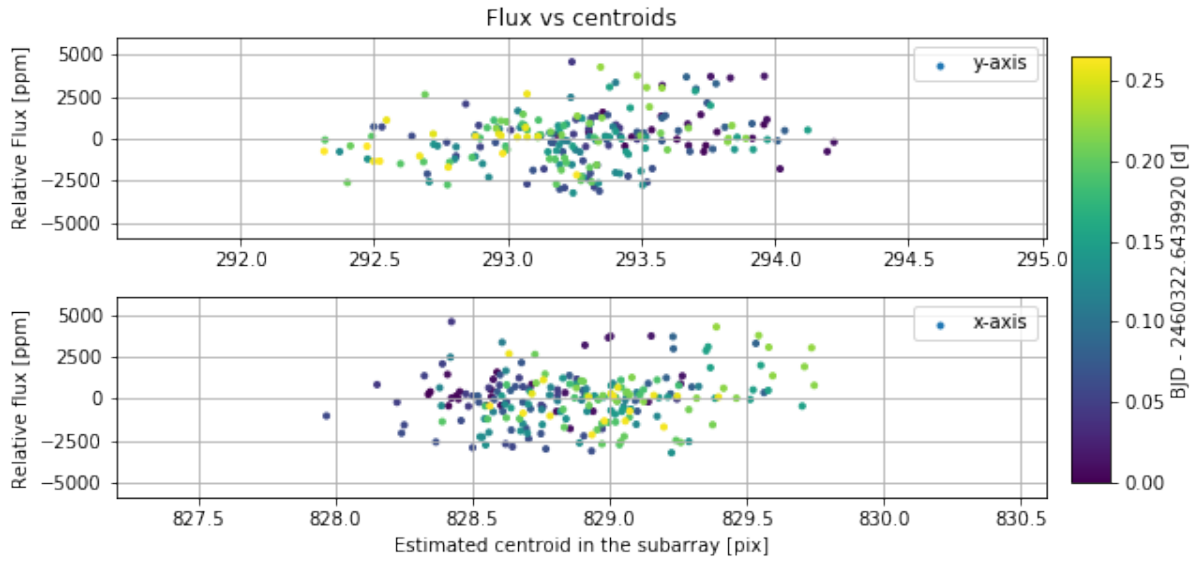


Figure 20. Flux as a function of the estimated centroid in the row (top) and column (bottom) directions. The points are clipped for better visualization.

	max -shift	max +shift	mean shift
Row	292.3	294.2	293.3
Column	828.0	829.7	828.9

Table 17. Maximum displacements of the estimated centroids in the row/column directions. The average displacement on each axis is also shown.

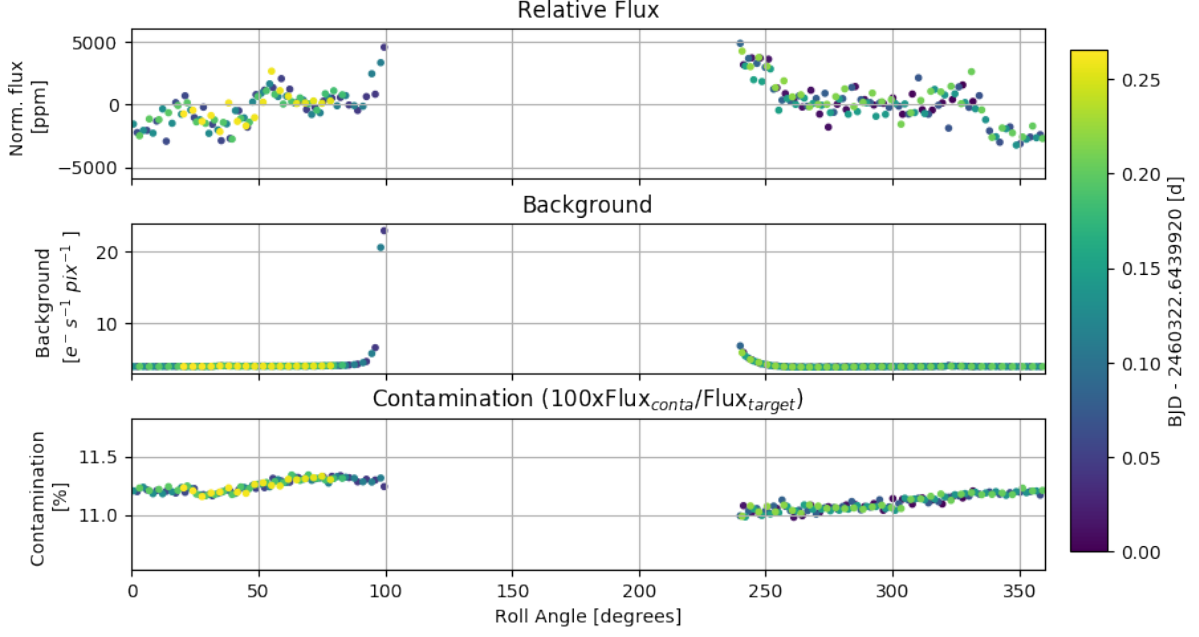


Figure 21. Relative flux ($R=25$ pix) as a function of the roll angle of the exposure (top). The estimated background (middle) and contamination (bottom) are also shown versus roll angle. Outliers are clipped for better visualization. Contamination details are described below in Section 3.11.

3.11 Contamination Estimation

Based on simulations of the observed Field of View (FoV), the DRP estimates the fraction of flux within the aperture which is induced only by background stars. Figure 22 shows the simulated FoV while Figure 23 shows the light curve (DEFAULT aperture) of the simulated FoV with only the background stars, i.e., with the target removed.

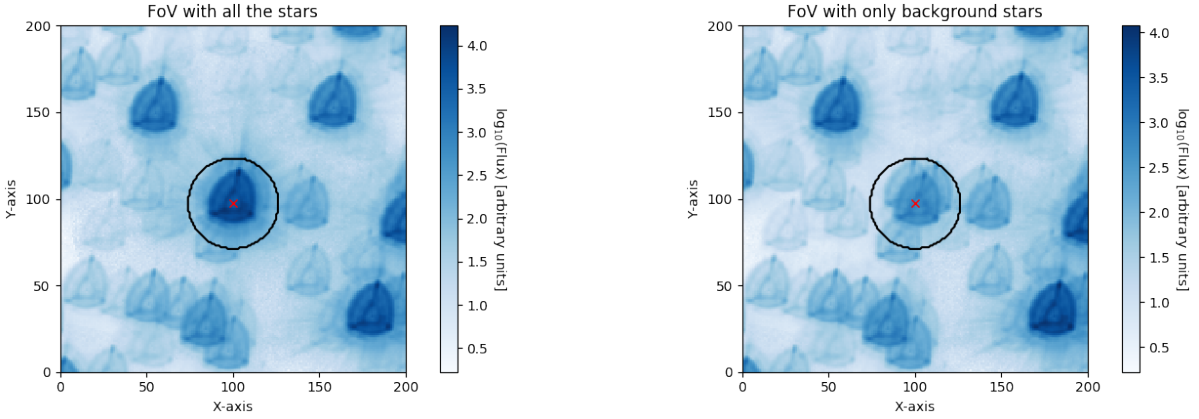


Figure 22. Images of the FoV extracted from the DRP simulations of the observation. Left: all the stars in the FoV are shown (target and background stars). Right: The target has been removed to show only the background stars in the FoV. The black circle and the red cross represent the default aperture and the target location, respectively.

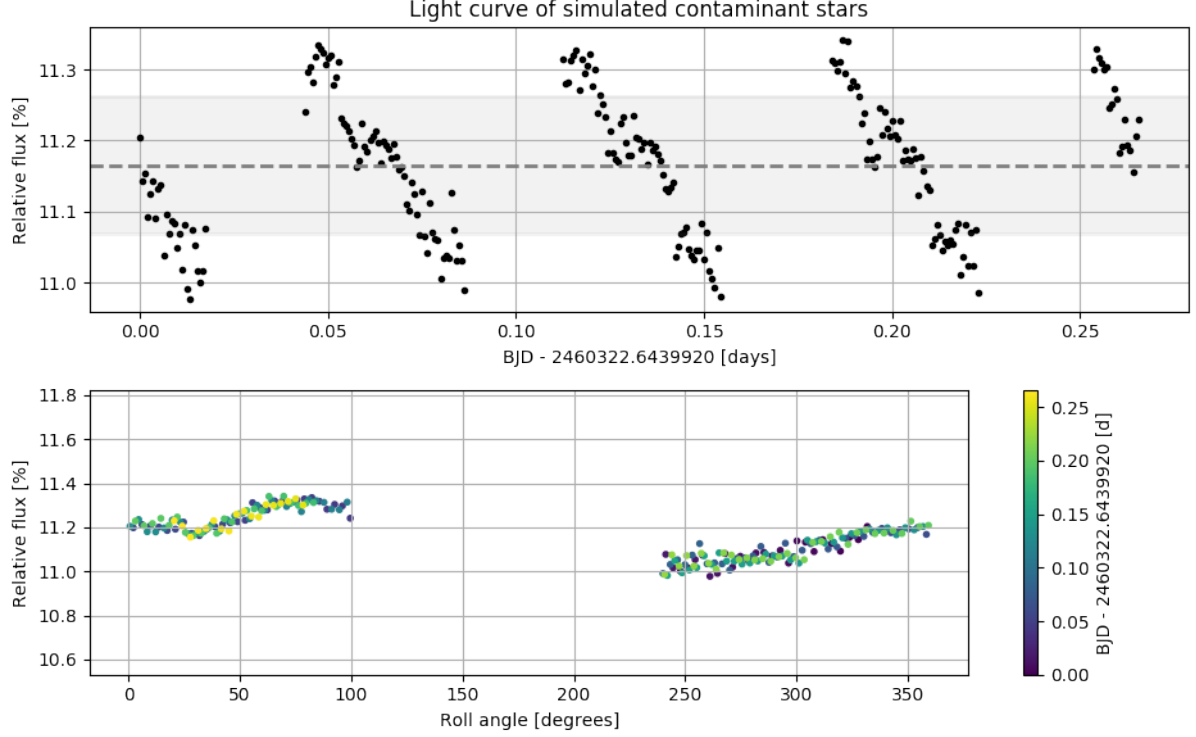


Figure 23. Flux of the simulated contaminant stars in the aperture (black points) as function of time (top panel) and roll angle (bottom panel) relative to the flux of the target. In the top panel, the mean of the contaminant flux (dashed line) and its standard deviation (shaded area) correspond to F_{cont} and σ_{cont} in the noise estimation of the photometry (see following section).

	mean [%]	RMS [%]
bkg stars flux	1.12e+01	9.69e-02

Table 18: Estimated mean and dispersion of the flux of contaminants in the DEFAULT aperture w.r.t the mean flux of the target.

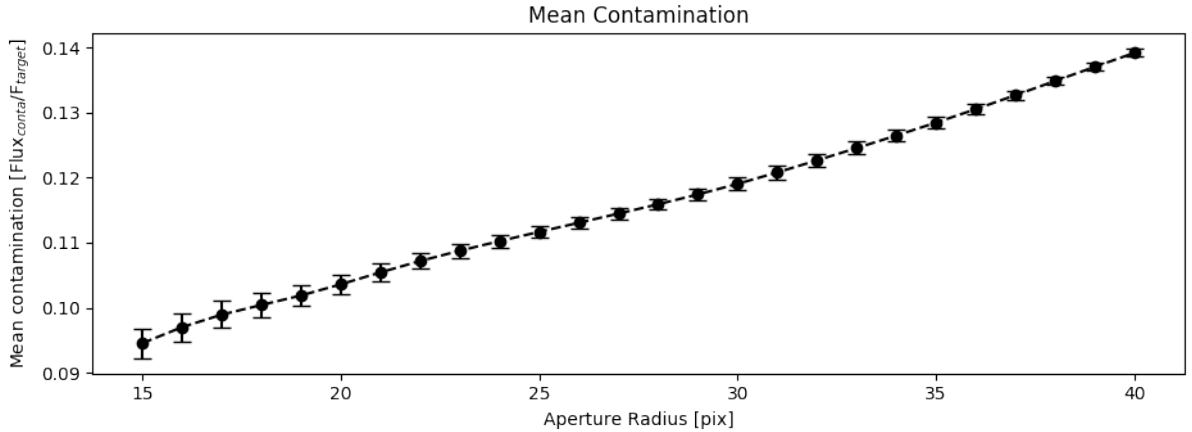


Figure 24. The mean contamination produced by background sources as a function of the aperture size. The values correspond to Flux of the contaminants in the aperture over the target's flux, both values estimated from the DRP simulations of the observed CHEOPS field of view (FoV). The error bars represent the RMS of the contamination variability produced by the rotation of the FoV (see Fig. 23). No intrinsic variability of the background sources has been included in the contamination estimations.

3.12 DRP Photometry

A quick summary of the metrics of the light curve for each aperture provided by the DRP is presented below. In general the metrics of the raw photometric time series and its point-to-point difference are provided. These numbers are also compared to the metrics obtained after applying a sigma-clipping filter.

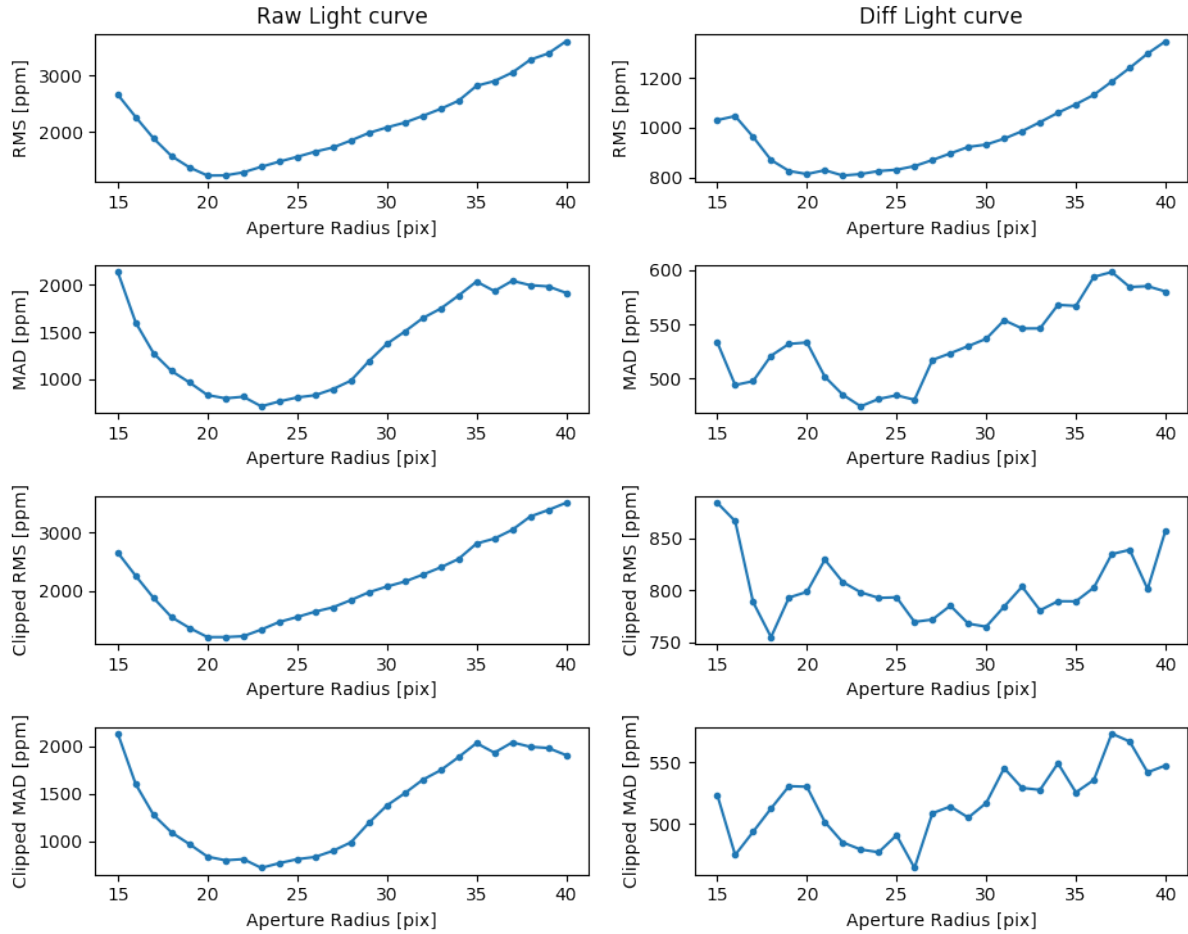


Figure 25. RMS and MAD of the raw light curve and the sigma-clipped version as a function of the aperture radii. The metrics are shown for the photometric time series as delivered by the DRP (left panels) and its point-to-point difference (right panels).

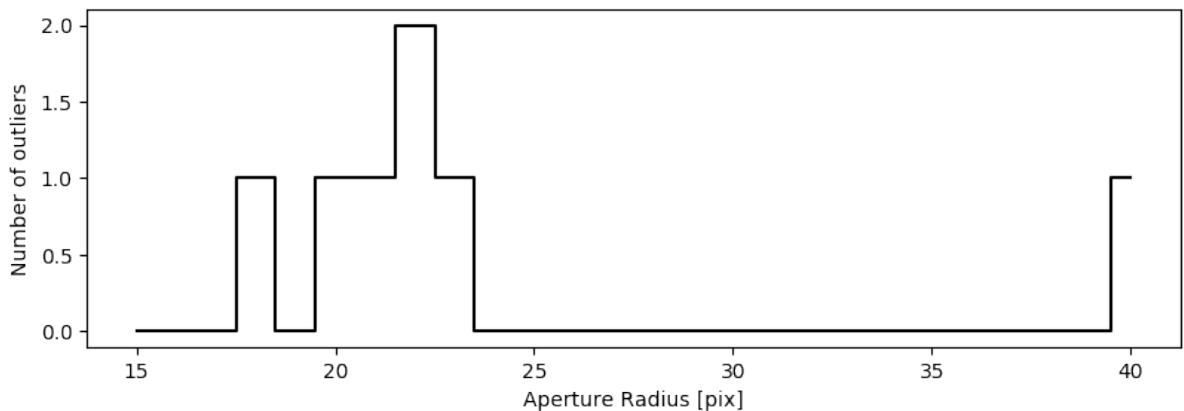


Figure 26. Number of outliers flagged in the light curve of each aperture radius.

As the metrics are sensitive of the number of high deviating points or outliers, below we present the metrics estimated when removing the same outlier points on each light curve. We compare two cases: one with the minimum and maximum number of outliers.

Minimum number of outliers: 0 (aperture R=15)
 Maximum number of outliers: 2 (aperture R=22)
 *Please note that several apertures can have the
 the same min/max number of outliers simultaneously.

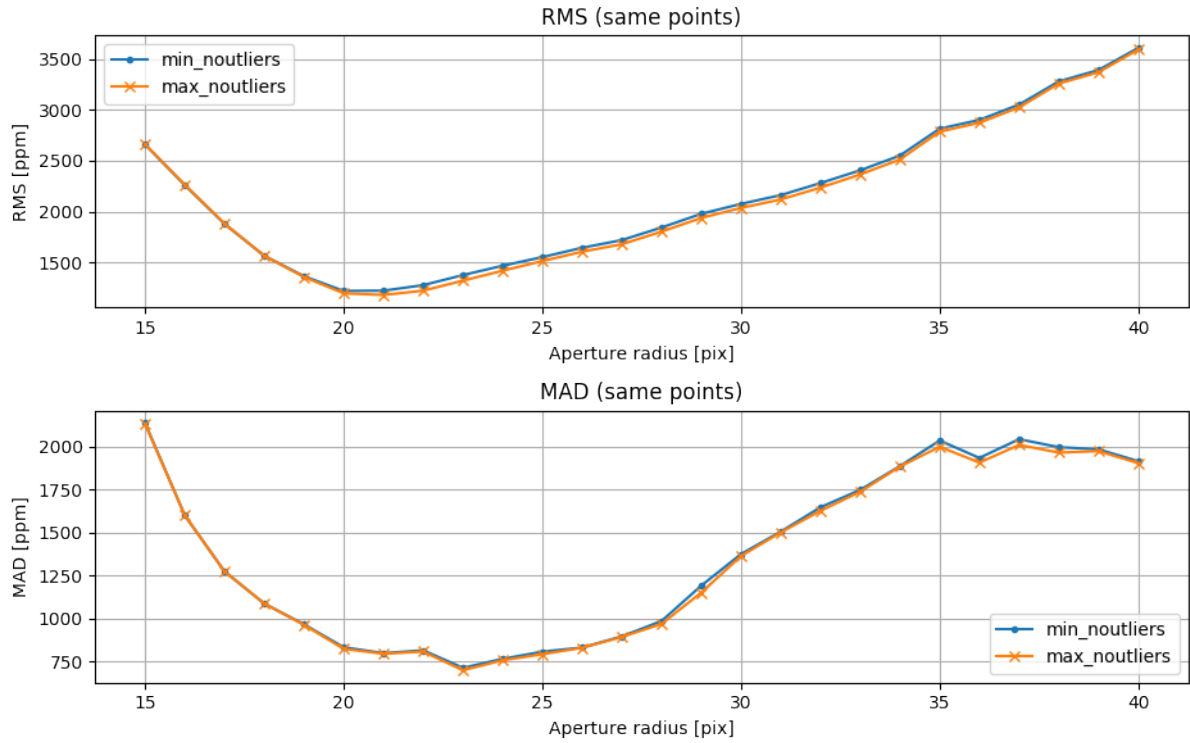


Figure 27. RMS (top) and MAD (bottom) computed by excluding the same photometric points in all the light curves. Two cases are shown, corresponding to the minimum (blue) and maximum number of outliers (yellow).

Below, the Fig. 28 shows the CDPP for 5, 10, 30 and 60* min as a function of the aperture size. * 60 minutes CDPP can be replaced by half of the visit duration in case of short visits.

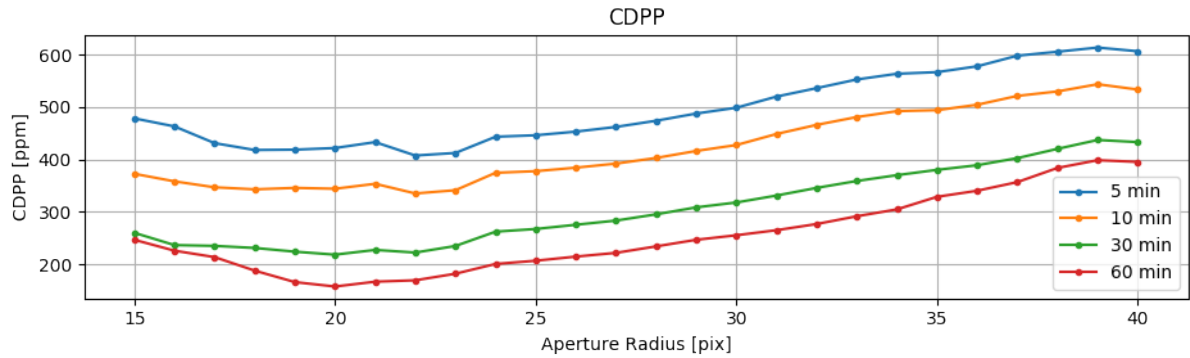


Figure 28. CDPP estimations as a function of the radius of the photometric aperture. The CDPP is estimated in time windows of 5, 10, 30 and 60* minutes.

The light curves with aperture size of R=[15, 20, 25, 30,35] pix are shown below in Figure 29.

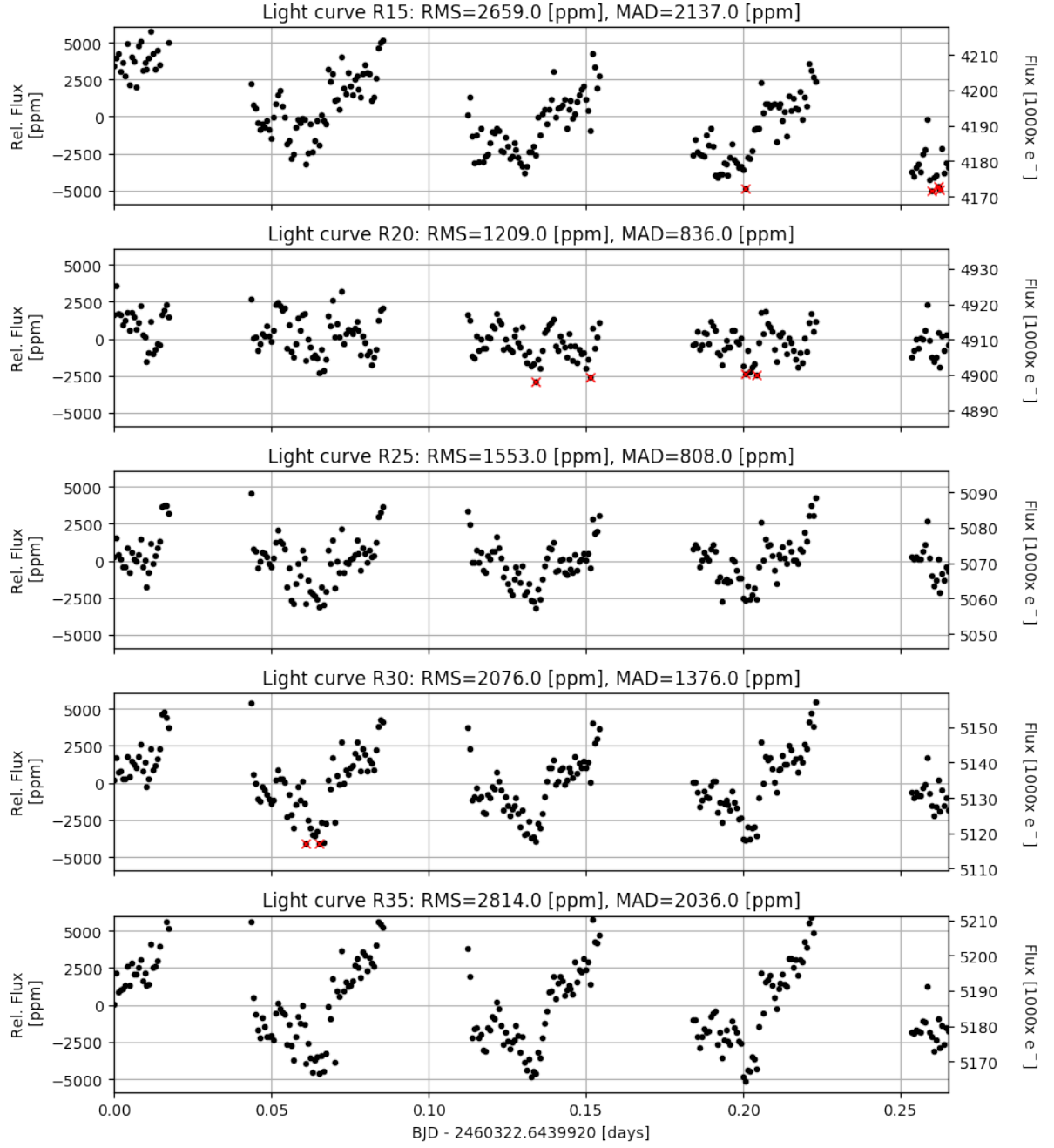


Figure 29. Light curves obtained by the DRP with apertures of radius $R=[15, 20, 25, 30, 35]$ pix. The sigma-clipped points of each light curve are marked with red-cross symbols. The RMS and MAD of each clipped light curve are reported on the top of each panel.

The Figure 30 represents another way to visualize the spread of the photometric points obtained with the different apertures. It shows the density distributions of the non-clipped points for every other light curve, starting with the smallest aperture $R=15$ pix.

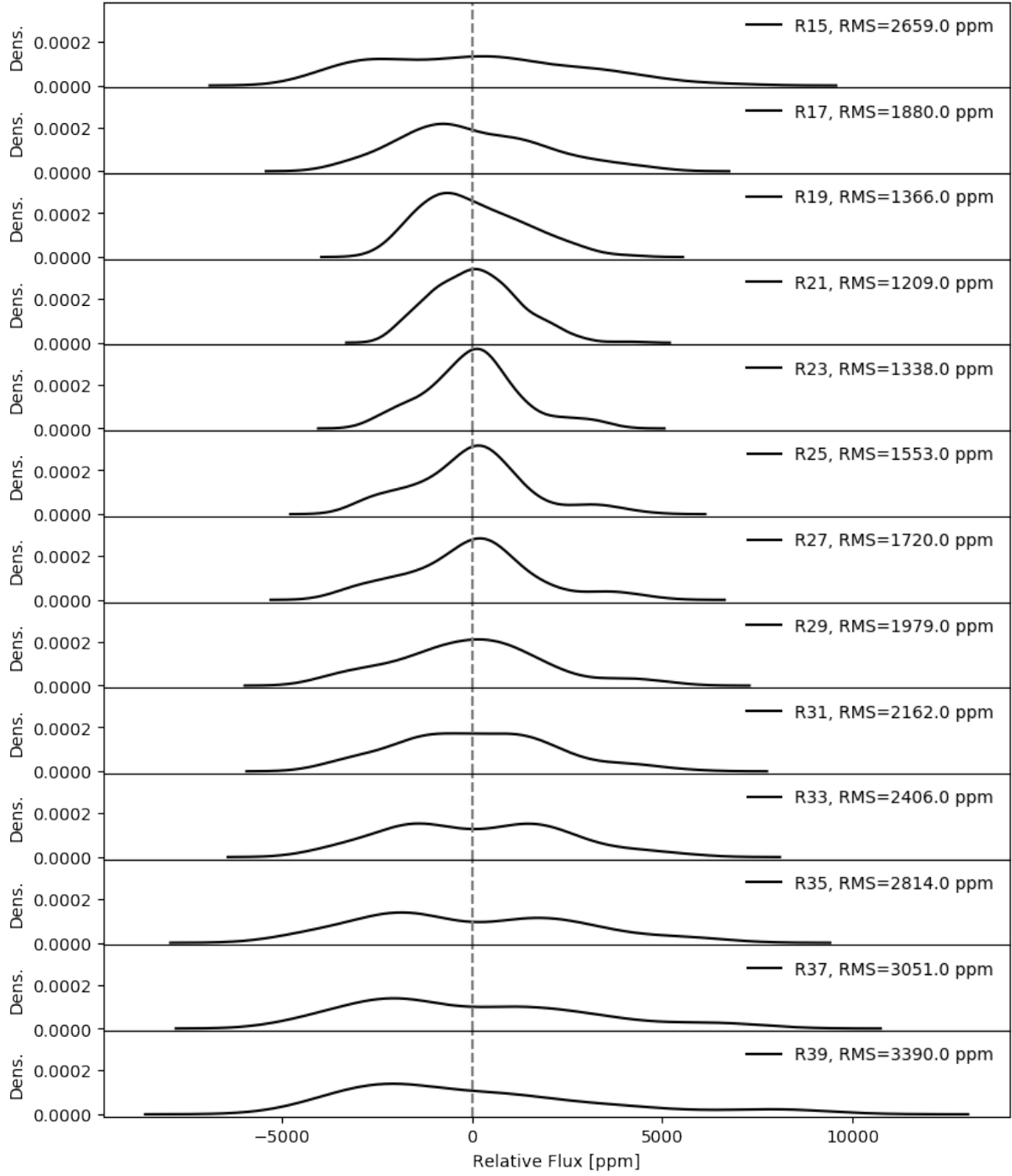


Figure 30. Density distributions the DRP light curves obtained using an aperture radius of $R=[15, 17, 19, 21, 23, 25, 27, 29, 31, 33, 35, 37, 39]$ pix.

	MAD [ppm]	RMS [ppm]	DIFF MAD [ppm]	CDPP10m [ppm]	CDPP3h [ppm]
R=15 [pix]	2137.3	2659.2	533.4	372.6	246.5
R=16 [pix]	1600.9	2259.9	493.9	358.2	225.7
R=17 [pix]	1274.9	1879.6	497.5	346.8	213.5
R=18 [pix]	1090.6	1549.6	520.9	343.0	187.6
R=19 [pix]	967.0	1365.6	531.9	345.7	165.7
R=20 [pix]	835.6	1208.9	533.2	344.1	157.3
R=21 [pix]	796.8	1209.3	501.6	353.5	166.5
R=22 [pix]	809.0	1223.9	485.0	335.1	169.2
R=23 [pix]	716.5	1337.7	474.2	341.3	181.7
R=24 [pix]	766.2	1468.6	481.0	374.6	200.4
R=25 [pix]	808.4	1553.5	484.4	377.6	206.6
R=26 [pix]	831.9	1645.2	480.3	384.4	214.4
R=27 [pix]	897.0	1720.3	517.0	392.1	221.6
R=28 [pix]	986.5	1844.3	523.2	402.9	234.0
R=29 [pix]	1192.2	1978.5	529.9	416.3	246.6
R=30 [pix]	1375.7	2075.8	536.6	427.6	255.3
R=31 [pix]	1506.1	2162.0	553.7	448.7	264.9
R=32 [pix]	1648.0	2280.3	546.1	466.1	276.7
R=33 [pix]	1749.1	2405.6	546.2	481.1	291.5
R=34 [pix]	1887.3	2550.5	568.0	492.3	304.7
R=35 [pix]	2036.1	2814.4	567.0	494.2	328.7
R=36 [pix]	1935.0	2900.5	593.8	504.6	340.3
R=37 [pix]	2044.0	3051.1	598.3	521.5	356.8
R=38 [pix]	1997.5	3279.0	584.5	530.0	383.9
R=39 [pix]	1984.6	3390.5	585.2	543.8	398.6
R=40 [pix]	1909.1	3515.3	580.3	533.6	395.3

Table 19. Metrics for each of the DRP light curves. The values of the aperture radius, the median absolute deviation (MAD), the point-to-point RMS and the Combined Differential Photometric Precision at 10 minutes (CDPP10m) and 3 hours (CDPP3h) are shown. 1 hour window is used if the visit duration is shorter than 3 hrs.

4 Appendix

4.1 Event flagging code

Below the code used to flag individual data points in the light curves

is shown. | The flag integer is represented as: |5|4|3|2|1|0|, where each digit corresponds to:

	Flag name	flag1	flag2	flag3
0	SAA	0: outside	1: inside	–
1	Temperature	0: within range	1: outside range (soft)	2: outside range (hard)
2	Earth Constraints	0: Straylight below threshold	1: Straylight above threshold	9: Earth occultation
3	Moon	0: above threshold	1: below threshold (soft)	2: below threshold (hard)
4	Sun	0: above threshold	1: below threshold (soft)	2: below threshold (hard)
5	Cosmic Rays	0: below threshold	1: >1% aperture contaminated	2: >5% image contaminated

Table 20. Code used for event flagging of the light curves data points. Moon and Sun flags correspond to relative angular separation thresholds.

4.2 Data Reduction Pipeline release log summary

Version 14.1

Release Date: 25 November 2022

- Dark Correction: using the M&C reference dark maps for the correction instead of a constant value.
- Cosmic Rays Detection/Correction: Bug fixes and fine tuning in the detection module. Fixed overcorrection.
- Hot Pixel detection: Detection after the dark map correction searching for surviving/new HPs. The HPs are not being corrected but the detection is transmitted in the DRP Bad Pixel Map (together with Dead and Telegraphic pixels).
- Multi-Aperture implemented. Moving/fixed aperture is allowed. Optimal aperture removed.
- DRP Report is updated accordingly.

Version 13.1

Release Date: 14 January 2021

- Incorporate the adoption by SOC of Gaia G mag for all the stars (including target) in the processing.
- Bias default values are now read directly from BIAS Reference file (values depend on CCD temperature).
- Mask implementation changed to use astropy regions. Mask areas of fixed apertures (RINF, RSUP, DE-FAULT) are constant between different visits.
- Fixed roll angle interpolation glitches.
- Minor changes in this DRP report.